
Are tunas relevant bioindicators of mercury concentrations in the global ocean?

Médieu Anaïs ^{1,*}, Lorrain Anne ¹, Point David ²

¹ IRD, Univ Brest, CNRS, Ifremer, UMR 6539, LEMAR, Plouzané, France

² Observatoire Midi-Pyrénées, GET, UMR CNRS 5563/IRD 234, Université Paul Sabatier Toulouse 3, Toulouse, France

* Corresponding author : Anaïs Médieu, email address : anais.medieu@gmail.com

Abstract :

Humans are exposed to toxic methylmercury mainly by consuming marine fish. The Minamata Convention aims at reducing anthropogenic mercury releases to protect human and ecosystem health, employing monitoring programs to meet its objectives. Tunas are suspected to be sentinels of mercury exposure in the ocean, though not evidenced yet. Here, we conducted a literature review of mercury concentrations in tropical tunas (bigeye, yellowfin, and skipjack) and albacore, the four most exploited tunas worldwide. Strong spatial patterns of tuna mercury concentrations were shown, mainly explained by fish size, and methylmercury bioavailability in marine food web, suggesting that tunas reflect spatial trends of mercury exposure in their ecosystem. The few mercury long-term trends in tunas were contrasted and sometimes disconnected to estimated regional changes in atmospheric emissions and deposition, highlighting potential confounding effects of legacy mercury, and complex reactions governing the fate of mercury in the ocean. Inter-species differences of tuna mercury concentrations associated with their distinct ecology suggest that tropical tunas and albacore could be used complementarily to assess the vertical and horizontal variability of methylmercury in the ocean. Overall, this review elevates tunas as relevant bioindicators for the Minamata Convention, and calls for large-scale and continuous mercury measurements within the international community. We provide guidelines for tuna sample collection, preparation, analyses and data standardization with recommended transdisciplinary approaches to explore tuna mercury content in parallel with observation abiotic data, and biogeochemical model outputs. Such global and transdisciplinary biomonitoring is essential to explore the complex mechanisms of the marine methylmercury cycle.

Keywords : Methylmercury, Minamata Convention, Biomonitoring, Spatial gradients, Temporal trends, Standardized monitoring guidelines

36 **1. Introduction**

37 Mercury (Hg) is a potent neurotoxin that poses health risks to the global population. It is
38 emitted into the environment from natural sources, but also originates from multiple anthropogenic
39 sources including atmospheric emissions and direct releases to land and water (Outridge et al., 2018).
40 Once released, Hg transport and fate is complex and influenced by chemical, physical, and biological
41 processes. Once deposited or taken up in the ocean, an expected substantial but yet not well defined
42 fraction of Hg is naturally transformed into the more toxic and bioavailable methylmercury (MeHg)
43 form (Bowman et al., 2020; Mason and Fitzgerald, 1990), which is easily absorbed by organisms and
44 can biomagnify along marine food webs. This compound also bioaccumulates within individuals over
45 time, resulting in higher MeHg concentrations in bigger fish. Humans are exposed to MeHg mainly by
46 their consumption of seafood (Sunderland et al., 2018), especially top predators like some tunas that
47 exhibit high MeHg concentrations relative to the rest of the food web (e.g., Bodin et al., 2017; Choy et
48 al., 2009; Houssard et al., 2019). The adverse effects of MeHg exposure on human and wildlife health
49 are well documented (Axelrad et al., 2007; Genchi et al., 2017), and MeHg health and socioeconomic
50 costs are estimated to be a billion dollars per year worldwide (Bellanger et al., 2013; Zhang et al., 2021).

51 Mercury is easily transported and deposited across national boundaries (Horowitz et al., 2017),
52 and thus requires international cooperation for its control. The United Nation Minamata Convention
53 on Mercury is a legally binding international agreement (ratified by 141 countries in June 2023,
54 www.mercuryconvention.org) with the objective of protecting human health and the environment
55 from anthropogenic Hg emissions and releases. This implies a mix of measures to control, reduce, and
56 eliminate major sources of Hg, but also an assessment of the resulting changes in emissions and
57 releases, and ultimately in human and ecosystem exposures. Given the complexity of the global Hg
58 cycle, such assessment of Hg changes in the environment requires a collection of metrics that
59 complement each other and capture different spatial and temporal dimensions of effectiveness.

60 In the atmosphere, a few long-term monitoring networks have been measuring air Hg
61 concentrations and deposition in contrasted regions of the world since the 1990s (Slemr et al., 2020,
62 2015; Zhang et al., 2016). Anthropogenic Hg emissions are thought to have tripled total Hg
63 concentrations in thermocline waters (100 – 1,000 m) of the global ocean relative to deeper older
64 waters (Lamborg et al., 2014), yet still unclear is how these anthropogenic Hg inputs are converted
65 into MeHg in oceans. Further developments of clean sampling protocols, and lower detection limits,
66 coupled to the establishment of global-scale oceanographic survey programs (i.e., CLIVAR and
67 GEOTRACES) in the past two decades, have led to more than 200 high-resolution and full depth profiles
68 of Hg speciation covering the Arctic, Atlantic, Pacific, and Southern Ocean (Bowman et al., 2020).
69 Although these measurements in the open ocean have improved our understanding of the
70 biogeochemical Hg cycle in the global ocean, they remain too scarce and limited in space and time to
71 evaluate the effectiveness of the Minamata Convention. To complement this abiotic monitoring,
72 bioindicators are commonly used for assessing environmental loads and associated ecological and
73 human health impacts resulting from controls on point sources.

74 An exemplary long-term biotic monitoring effort is being conducted by the Arctic Council's
75 Arctic Monitoring and Assessment Program (AMAP), and involves Hg measurements in fishes, birds,
76 marine mammals, and people to complement Hg observations in air and seawater (AMAP, 2021).
77 Atmospheric Hg levels in the Arctic are generally decreasing, while both increasing and decreasing
78 trends of Hg in Arctic biota have been observed over the last decades. These contrasted trends likely

79 result from concomitant reducing Hg emissions from North America and Europe, and/or climate-
80 induced confounding factors (e.g., thawing permafrost, melting glaciers, and changes to vegetation
81 cover) altering Hg uptake and re-emission (Jiskra et al., 2020), and MeHg production/degradation and
82 biomagnification in upper predators (Masbou et al., 2015; Point et al., 2011; Wang et al., 2019). In the
83 meantime, there are very few long-term Hg biomonitoring efforts in tropical regions, while populations
84 from these regions are often considered as vulnerable regarding Hg exposure given that seafood
85 represents their primary source of animal proteins (Bell et al., 2009; Béné et al., 2015). In tropical
86 marine ecosystems, tunas have been identified as potential human and ecological health bioindicators
87 (UN Environment, 2019). There is indeed a consensus that tunas can pose concern for human exposure
88 to MeHg as they are one of the most important global sources of seafood (FAO, 2018), while MeHg
89 represents the major chemical form of total Hg in muscle (> 90 %) (Houssard et al., 2019; Mergler et
90 al., 2007). There is yet no evidence that tunas are direct relevant bioindicators species of Hg
91 concentrations in the ocean, i.e., that they are able to reflect Hg exposure in their ecosystem,
92 integrating local and global Hg source mixing and oceanic transformation into MeHg over different
93 spatial and temporal scales.

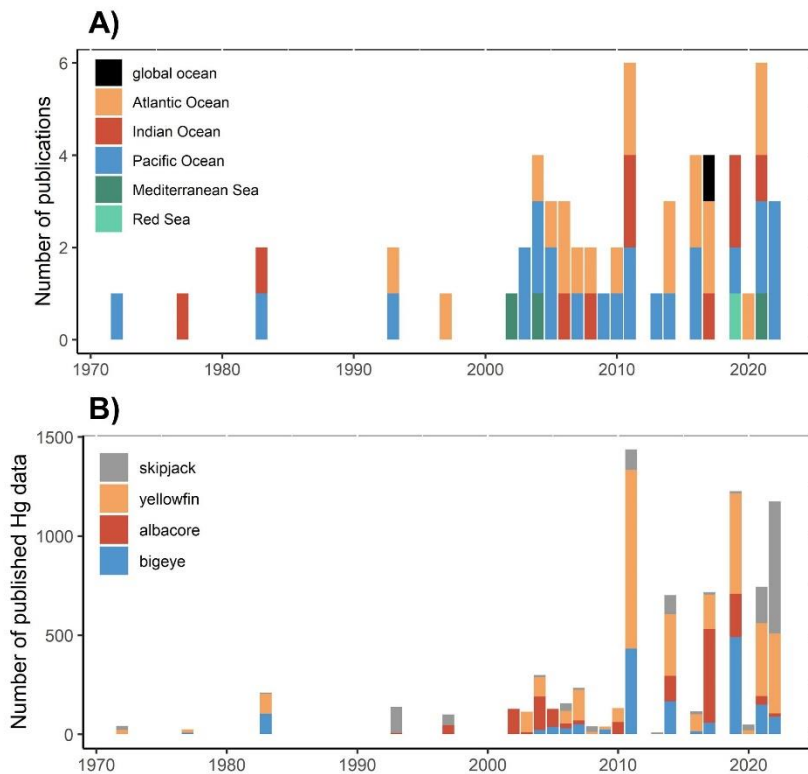
94 This article reviews information from the literature to investigate the relevance of tunas as Hg
95 bioindicators in the ocean for the Minamata Convention, focusing on muscle, the recommended
96 matrix to biomonitor MeHg exposure in fishes with a high percent MeHg like tunas (UN Environment,
97 2019). While the term “tunas” refers to 15 different ocean fish species, including seven of commercial
98 importance, this review focuses only on the four worldwide-distributed species to ensure
99 comparability of Hg exposure and accumulation at both regional and global scales. This includes the
100 three tropical tunas, i.e., bigeye (*Thunnus obesus*), yellowfin (*T. albacares*), and skipjack (*Katsuwonus*
101 *pelamis*), and albacore (*T. alalunga*, a temperate and tropical species). Although classified as highly
102 migratory, we hypothesize that tropical tunas, and to a lesser extent albacore, are suitable to explore
103 high resolution subregional patterns of marine MeHg bioavailability and accumulation as these species
104 are suspected to display relative site fidelity (Fonteneau and Hallier, 2015; Houssard et al., 2017)
105 contrary to Pacific (*T. orientalis*), Atlantic (*T. thynnus*) and Southern (*T. maccoyii*) bluefin tunas that
106 undergo large transoceanic migrations (Block et al., 2005; Hobday et al., 2015; Madigan et al., 2014).
107 Tropical tunas and albacore are also widely exploited (representing 99 % of the global tuna catches)
108 (ISSF, 2021), and monitored by regional fishery management organizations through several sampling
109 programs. Given this context, these four species represent a possible gold mine of biological samples
110 to generate robust and comparable datasets, a mandatory requirement to get accurate and sensitive
111 temporal and spatial Hg biomonitoring studies in the global ocean. While focussing on these four tuna
112 species, some results on bluefin tunas are also presented as they bring valuable information, not
113 available for tropical species nor albacore, to discuss the relevance of tunas as bioindicators of Hg in
114 the ocean.

115

116 **2. State of mercury data in tunas**

117 Since the 1970s, more than 50 studies have documented Hg concentrations in tropical tunas
118 and albacore. These studies were conducted mainly in the Pacific ($n = 26$) and in the Atlantic Oceans
119 ($n = 20$), and to a lesser extent in the Indian Ocean ($n = 10$) (Figure 1A; SI Appendix Table S1). Only one
120 study has documented Hg concentrations for the global ocean for yellowfin (Nicklisch et al., 2017).
121 Yellowfin is indeed the most studied tuna species regarding its Hg concentrations (number of

122 individuals with published Hg concentration, $n = 3,423$), followed by bigeye ($n = 1,674$), albacore ($n =$
 123 $1,435$), and skipjack ($n = 1,420$) (Figure 1B). Mercury levels were found to vary among tuna species,
 124 but also in space and time, as discussed in the three following sections, respectively, regarding the
 125 expected objectives of Hg biomonitoring in the open ocean.

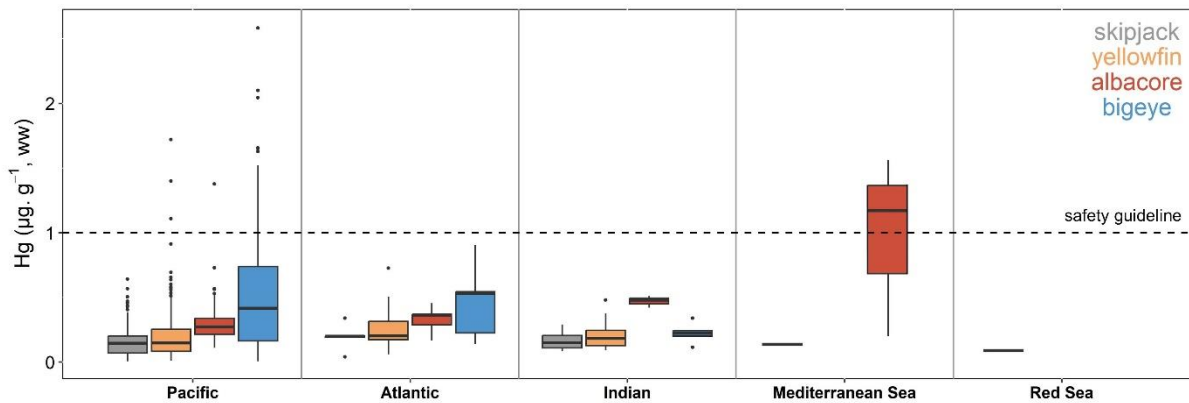


126

127 **Figure 1. Review of published mercury data in tunas through time. A)** Number of publications per year and
 128 ocean documenting mercury (Hg) concentrations in muscle tissues of tropical tunas and albacore. **B)** Number of
 129 Hg concentration data reported in publications per year and tuna species. References and detailed information
 130 used to produce these histograms are reported in SI Appendix Table S1.

131 **3. Inter-species differences in tuna mercury concentrations**

132 Mercury concentrations have been shown to differ among tuna species (Figure 2). While
133 bigeye, albacore, and yellowfin can display Hg concentrations exceeding the food safety guidelines of
134 $1 \mu\text{g}\cdot\text{g}^{-1}$ wet weight (FAO Codex Alimentarius Commission, 2021), skipjack samples always show Hg
135 levels below the limit (Figure 2; SI Appendix Table S1). Samples with Hg concentrations exceeding the
136 food safety guidelines are generally associated to bigger individuals, illustrating the natural
137 bioaccumulation of Hg in organisms through time, and the consequent need to consider both tuna
138 species and fish size when addressing recommendations in terms of food safety regarding Hg content.



139 **Figure 2. Gradient of mercury concentrations in tropical tunas and albacore.** Boxplots illustrate the inter-species
140 variability of mean total mercury (Hg) concentrations ($\mu\text{g}\cdot\text{g}^{-1}$, wet weight) measured in white muscle tissue of
141 skipjack (grey), yellowfin (orange), albacore (red), and bigeye (blue) caught in the Pacific, Atlantic, and Indian
142 Oceans, and in the Mediterranean Sea and the Red Sea. The dashed line represents the food safety guideline of
143 $1 \mu\text{g}\cdot\text{g}^{-1}$ wet weight. Thick bars are the median values, points are outliers, and the boxes contain 50% of the data.
144 References and detailed information used to produce these boxplots are reported in SI Appendix Table S1.
145

146 Relative differences of Hg concentrations among tuna species are consistent among study
147 regions of the global ocean, following this general pattern in Hg concentrations: bigeye > albacore >
148 yellowfin and skipjack (Blum et al., 2013; Bodin et al., 2017; Choy et al., 2009; Garcia et al., 2007;
149 Houssard et al., 2019; Médieu et al., 2021a, 2021b; Yamashita et al., 2005). The highest Hg
150 concentrations in bigeye compared to the three other species is presumably the result of three
151 confounding factors: i) a higher trophic position of this species, ii) a deeper vertical habitat facilitating
152 its access to mesopelagic prey with enhanced Hg concentrations, and iii) a longer lifespan (Choy et al.,
153 2009; Ferriss and Essington, 2011; Houssard et al., 2019). Tropical tunas and albacore indeed display
154 distinct growth rates (i.e., skipjack > yellowfin > albacore > bigeye), lifespan (i.e., skipjack < yellowfin <
155 albacore < bigeye), vertical habitats (bigeye generally dive deeper than the epipelagic skipjack and
156 yellowfin), and diet preferences, which may also vary among ocean basins (Murua et al., 2017; Olson
157 et al., 2016; Pethybridge et al., 2018). Further investigation at the global scale remains needed to
158 disentangle the relative importance of these ecological and biological processes, alongside the natural
159 marine biogeochemical functioning, to explain the inter-species differences of tuna Hg concentrations.
160 Yet, these preliminary results shed light on the potential power of combining these four tuna species
161 to investigate both horizontal and vertical variability of MeHg bioavailability in the water column, and
162 MeHg biomagnification pathways along pelagic food webs.

163
164

4. Spatial variability of mercury concentrations in tunas

Within a same tuna species, Hg concentrations also vary among ocean regions (Figure 3). Despite the scientific interest and the social and economic needs to document Hg variability in the global ocean, the vast majority of studies available to date have been conducted on a small spatial scale, relying most of the time on imprecise tuna catch locations (Figure 4A). Since the 2010s, regional collaborations and exchange of tuna Hg data associated to precise tuna catches enabled highlighting regional differences in Hg concentrations in yellowfin and bigeye tunas from the eastern Pacific Ocean (Figure 4C) (Ferriss and Essington, 2011), and in albacore from the western Indian Ocean (Chouvelon et al., 2017). In the global ocean, an eightfold difference in Hg concentrations was documented in yellowfin samples among 12 different locations (Nicklisch et al., 2017). Here, our compilation of all Hg data in tropical tunas and albacore from the global ocean reveals that mean observed Hg concentrations vary across sites by a factor 64 (0.01 – 0.64 $\mu\text{g}\cdot\text{g}^{-1}$, wet weight, min-max), 172 (0.01 – 1.72 $\mu\text{g}\cdot\text{g}^{-1}$), 14 (0.11 – 1.56 $\mu\text{g}\cdot\text{g}^{-1}$), and 258 (0.01 – 2.58 $\mu\text{g}\cdot\text{g}^{-1}$) in skipjack, yellowfin, albacore, and bigeye, respectively (Figure 3). These species-specific and global-scale compilations confirm that Hg concentrations are highly variable among species and sites. They also highlight that the vast majority of the studies documenting Hg concentrations in tunas rely on spot samples acquired at low spatial resolution, which do not allow exploring regional spatial patterns of Hg exposure and accumulation in pelagic biota. Recently, international collaborations and access to tuna samples from extensive tuna tissue banks have enabled to produce broad-scale and high-resolution maps of Hg concentrations in bigeye, yellowfin, and albacore from the western central Pacific region (Houssard et al., 2019) (Figure 4E), and in skipjack for the entire Pacific Ocean (Médieu et al., 2022). Such maps allow refining the assessments of risk exposure to Hg associated with human consumption according to tuna species and tuna catch areas.

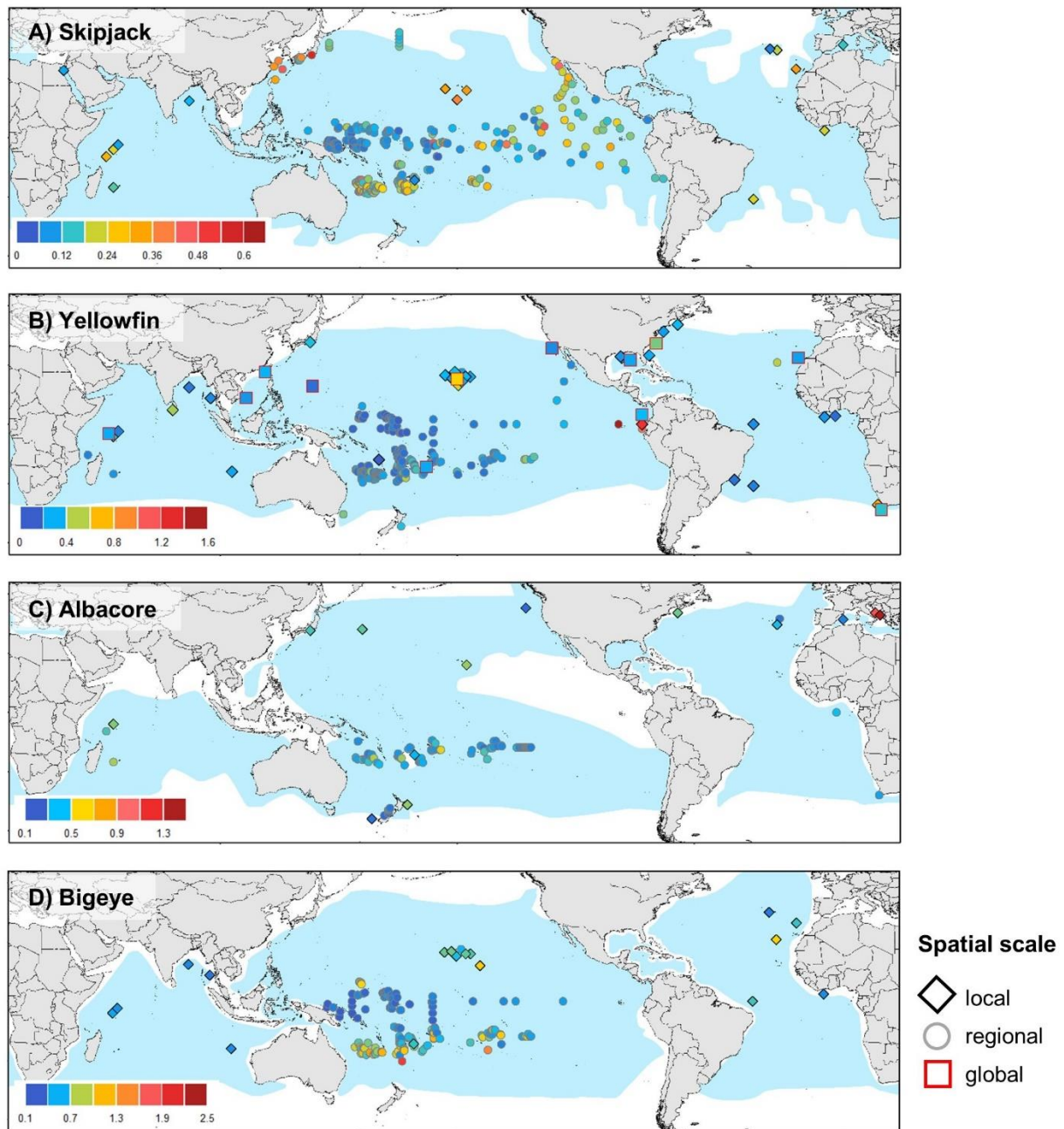
In most of the low resolution spatial studies, fish body size or weight has been identified as the best predictor of intra-species variability of tuna Hg concentrations, illustrating the natural bioaccumulation property of Hg in individuals over time (Figure 4B) (e.g., Besada, 2006; Boush and Thieleke, 1983; Cai et al., 2007; Chen et al., 2014, 2011; Kojadinovic et al., 2007; Peterson et al., 1973; Rivers et al., 1972; Sompongchaiyakul et al., 2008; Teffer et al., 2014). Yet, this body size/weight effect is not often considered when comparing tuna Hg concentrations at regional scales. For instance, between Hawaii and the North East Pacific Ocean, Nicklisch et al. (2017) reported a 4-fold increase of Hg concentrations in yellowfin (mean total Hg = 0.602, and 0.154 $\mu\text{g}\cdot\text{g}^{-1}$, ww, respectively), but a two-fold difference of size (mean standard length = 117 and 56 cm, respectively). The use of quantitative methods (e.g., mixed effects in multiple regression models) can help account for the body size effect and quantify its relative importance compared to regional effects when exploring the regional variability of tuna Hg concentrations. In the eastern Pacific Ocean, such an approach revealed higher Hg concentrations in bigeye in the eastern equatorial region than in Hawaii, central- and mid-equatorial Pacific, not explained by fish size differences (Figure 4D) (Ferriss and Essington, 2011). Recently, length-standardization methods of tuna Hg concentrations have been developed to remove the bias associated to fish size differences among individuals, and to characterize the natural bioaccumulative properties of Hg in tunas when exploring Hg spatial patterns (see methodological details in section 6.2.) (Houssard et al., 2019; Médieu et al., 2022). This method revealed that differences in tuna sizes explained high observed Hg concentrations in bigeye in the equatorial western Pacific, but not in the southwestern region where standardized Hg concentrations remained highest than in any other region (Figure 4E & F) (Houssard et al., 2019). In the literature, individual fish length

209 is rarely reported alongside individual tuna Hg concentration, which prevents us from standardizing
210 most of the published Hg concentrations with this method, and producing compilation maps of
211 standardized Hg concentrations in the four tuna species. Contrary to a simple comparison of observed
212 Hg concentrations measured in different locations (Figure 3), mapping standardized Hg concentrations
213 at a high resolution and broad spatial scale allows exploring the spatial distribution of Hg
214 concentrations anomalies not explained by Hg bioaccumulation and fish sizes among individuals, but
215 likely due instead to other processes such as tuna trophic ecology, ocean biogeochemistry or
216 anthropogenic Hg emissions.

217 Identifying and evaluating the relative importance of these underlying processes, other than
218 body size effect, to explain spatial patterns of tuna Hg levels can be complicated given the difficulty
219 with quantifying these processes, and disentangling possible interplay among them. Tuna foraging
220 depth is considered as a key driver to explain higher Hg concentrations in mesopelagic species like
221 bigeye (Choy et al., 2009); yet still unclear is the relative importance of both food chain length and/or
222 baseline Hg variations as possible causal effects (Ferriss and Essington, 2011). The recent exploration
223 of standardized Hg concentrations in tunas alongside ecological data (e.g., tuna trophic position
224 estimates), biogeochemical (e.g., dissolved O₂ concentrations), physical (e.g., thermocline depth), and
225 anthropogenic (e.g., atmospheric elemental Hg concentrations) model outputs through quantitative
226 models (e.g., generalized additive models) offers new perspectives to disentangle the relative
227 importance of ecological, biogeochemical and anthropogenic processes. In the western central Pacific
228 Ocean, this transdisciplinary approach revealed that spatial variability of standardized Hg
229 concentrations in bigeye, yellowfin, and albacore were mainly related to tuna foraging depth and local
230 ocean biogeochemistry, and that spatial trophic changes were of minor importance (Houssard et al.,
231 2019). Similarly, large spatial patterns of standardized Hg concentrations in the epipelagic skipjack
232 were mainly explained by the natural functioning of the Pacific Ocean, likely via variations in the MeHg
233 concentrations and the depth at which MeHg peaks within the water column (Médieu et al., 2022). In
234 this latter study, authors also revealed the local influence of anthropogenic emissions in Asia,
235 enhancing skipjack Hg concentrations in the northwestern Pacific Ocean. Overall, these two broad-
236 scale and transdisciplinary studies lead to the hypothesis that the spatial variability in tuna Hg
237 concentrations is mainly explained by both tuna foraging depth and the vertical and horizontal
238 variability of MeHg bioavailability in the ocean. These results shed light on the potential power of
239 combining tropical tunas and albacore to investigate both horizontal and vertical variability of MeHg
240 bioavailability in the water column, and MeHg biomagnification pathways along pelagic food webs.
241 These findings call for deeper global comparisons with observed Hg data in the ocean.

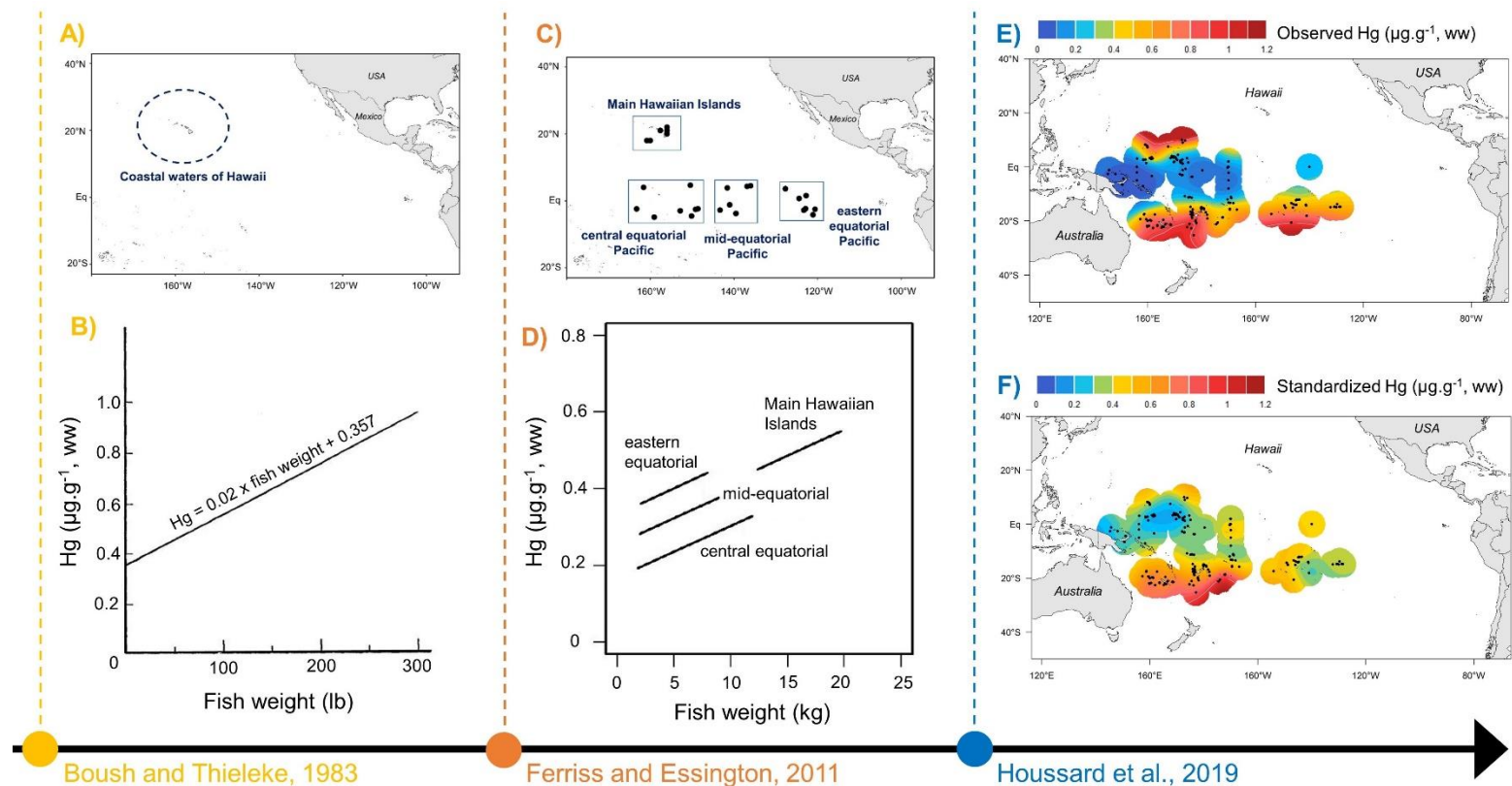
242 Such comparisons are rarely achievable because of the mismatch in space and time between
243 available tuna Hg data and scarce observations of Hg concentrations and speciation in the ocean. In
244 the southwestern Pacific Ocean, Hg concentrations in tropical tunas and albacore were recently shown
245 to mirror ambient seawater MeHg concentrations, with higher Hg concentrations in the mesopelagic
246 bigeye reflecting higher dissolved MeHg concentrations in subsurface waters (Barbosa et al., 2022). At
247 the global scale, Hg concentrations in bluefin tunas were also found to reflect global patterns of Hg
248 bioavailability and pollution in each ocean basin (Tseng et al., 2021). Together, these results exploring
249 Hg concentrations in tunas in parallel with global and high-resolution model outputs, or with dissolved
250 MeHg observations, confirm that tunas tend to reflect global and regional changes of Hg exposure in
251 their ecosystem. In the framework of the Minamata Convention, such coupled approaches could
252 benefit the general understanding of Hg accumulation in tunas in the global ocean, and could therefore

253 offer perspective in modelling responses of Hg concentrations in marine top predators to changes in
254 oceanic MeHg concentrations in the context of different emissions scenarios.



255

256 **Figure 3. Review of mercury concentrations in tropical tunas and albacore in the global ocean.** Spatial
257 variability of total mercury (Hg) concentrations ($\mu\text{g}\cdot\text{g}^{-1}$, wet weight) in white muscle tissue (coloured symbols)
258 and potential habitat distribution (light blue) of **A)** skipjack, **B)** yellowfin, **C)** albacore, and **D)** bigeye at the
259 global scale. The colour of symbols refers to total Hg concentrations measured in tuna muscle samples. The
260 shape of symbols refer to the spatial scale of the studies from which tuna Hg data originate: the 12 squares
261 represent the 12 samples locations used in the unique global study (Nicklisch et al., 2017), the circles are the
262 locations used in regional studies (Chen et al., 2011; Chauvelon et al., 2017; Endo et al., 2016; Ferriss and
263 Essington, 2011; Garcia-Vazquez et al., 2021; Houssard et al., 2019; Kojadinovic et al., 2006; Médiéu et al.,
264 2022; Ordiano-Flores et al., 2011; Yamashita et al., 2005), and the diamonds represent locations where tuna Hg
265 concentrations are reported in local studies. Potential habitat distributions per species were obtained from the
266 IUCN Red List Spatial Data of tunas (IUCN, 2017). References and detailed information used to produce these
267 maps are reported in SI Appendix Table S1.



268

269 **Figure 4. Temporal evolution of the research effort to document mercury accumulation in tunas.** Different sampling strategies and standardization methods to investigate
 270 mercury (Hg) concentrations in bigeye in the Pacific Ocean. In the 1980s, **A)** bigeye samples were reported at a rough spatial resolution (i.e., coastal waters of Hawaii
 271 symbolised by the dashed circle), and **B)** Hg concentrations ($\mu\text{g}\cdot\text{g}^{-1}$, wet weight) in bigeye were found to increase linearly with individual fish weight illustrating the natural
 272 bioaccumulation of Hg through time, adapted from Boush and Thieleke (1983). In the beginning of 2010s, **C)** precise catch locations were provided for each bigeye samples
 273 (black dots), allowing to investigate **D)** differences of Hg bioaccumulation patterns (black lines) in bigeye among four regions of the eastern Pacific Ocean, adapted from
 274 Ferriss and Essington (2011). In the late 2010s, a large and high-resolution compilation of Hg data in bigeye samples (black dots) allowed to map **E)** large spatial differences
 275 of bigeye Hg concentrations ($\mu\text{g}\cdot\text{g}^{-1}$, wet weight) in the western central Pacific Ocean. Moreover, robust standardization methods of Hg concentrations to individual fish
 276 length helped removing bias associated to different individual fish sizes and revealing **F)** large spatial differences of standardized Hg concentrations (at 100 cm fork length,
 277 $\mu\text{g}\cdot\text{g}^{-1}$, wet weight) in bigeye in the western central Pacific Ocean, not explained by natural Hg bioaccumulation through time, but rather by ecological and/or
 278 biogeochemical processes, adapted from Houssard et al., (2019).

279 5. Temporal variability of mercury concentrations in tunas

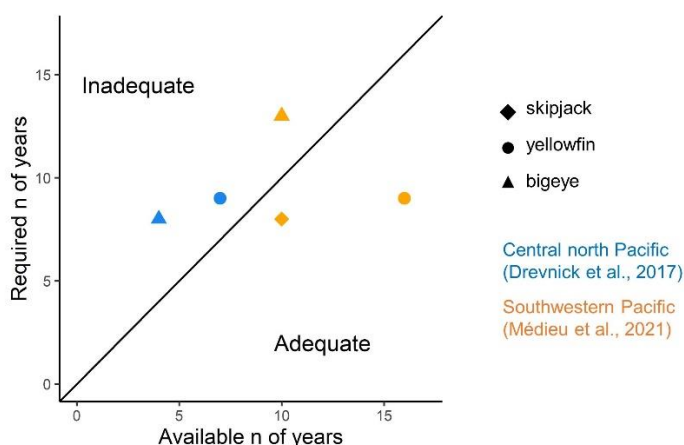
280 Another key aspect when evaluating the relevance of tunas as bioindicators for the Minamata
281 Convention is their ability to reflect temporal changes of Hg trends and inputs to the environment at
282 both local and global scales. Only four temporal studies of Hg concentrations are available to date in
283 tropical tunas, plus one in Atlantic bluefin, all showing distinct results regarding Hg long-term trends.
284 In the central north Pacific Ocean (i.e., Hawaii), stable Hg concentrations were found in yellowfin and
285 bigeye between the 1970s and the 1990s (Kraepiel et al., 2003). A re-evaluation of these stable trends
286 in the light of new data showed increasing Hg concentrations in yellowfin ($+ 5.5 \pm 1.6$ %/year during
287 1998-2008), and in bigeye ($+ 3.9 \pm 2.1$ %/year during 2002-2008), which were suggested to result from
288 an increasing transport and deposition of anthropogenic Hg, as well as the lateral flow of water masses
289 from the north west Pacific (Drevnick et al., 2015; Drevnick and Brooks, 2017). Conversely, Lee et al.
290 (2016) reported an annual decrease of Hg content of 0.018 ± 0.003 % between 2004 and 2012 in
291 Atlantic bluefin from the northwestern Atlantic Ocean, which was assumed to reflect a reduction in
292 North American Hg emissions. Unfortunately, no complementary trophic ecology data were available
293 in these studies to discuss if confounding temporal changes in tuna diet could contribute to the
294 contrasted temporal trends of Hg content, and potentially biased the response of tuna Hg burden to
295 changes of anthropogenic releases to the environment. In the southwestern Pacific (i.e., New
296 Caledonia and Fiji), the evaluation of Hg concentrations in the three tropical tunas between 2001 and
297 2018, alongside ecological data (i.e., nitrogen and carbon stable isotopes), revealed inter-annual
298 variability but no significant long-term trends of both tuna diet and tuna Hg concentrations (Médiéu
299 et al., 2021). The absence of temporal trends in tuna Hg concentrations in the southwestern Pacific
300 contrasts with the other available temporal studies in tunas from the northern hemisphere (Drevnick
301 et al., 2015; Drevnick and Brooks, 2017; Lee et al., 2016), and the increasing trend of Hg emissions
302 reported for the southern hemisphere since the 1980s (Streets et al., 2017). Conversely, it is in
303 accordance with low and stable anthropogenic Hg emissions into the atmosphere from Oceania
304 (Streets et al., 2019). Such disconnect between estimated regional variations in emissions and
305 deposition and stable Hg concentrations in biota has been documented in other marine and freshwater
306 ecosystems (Wang et al., 2019), and likely result from two main confounding factors: i) the large
307 quantities of legacy Hg that remain available for bioaccumulation, and ii) changes occurring in multi-
308 causal, local, and regional processes (e.g., climate) that control the speciation, bioavailability, and
309 bioaccumulation of both current and legacy emitted Hg.

310 Differences of temporal trends in tuna Hg concentrations could also result from the
311 operational difficulty of getting robust and continuous datasets over long periods of time to determine
312 sensitive and accurate Hg time series. In the framework of AMAP, several metrics of performance have
313 been developed to describe and discuss the statistical power of Hg time series, and ensure statistically
314 powerful Hg biomonitoring through time in the Arctic (AMAP, 2021). Among them, the “adequacy” has
315 been developed to compare the time series ability to detect trends and at the same time indicate
316 whether trend detection is justified for the time series (Bignert et al., 2004). It is defined as the number
317 of actual monitoring years in a time series divided by the number of years of sampling required to
318 detect a 5 % annual change in Hg concentrations. A ratio ≥ 1 implies that the time series are adequate.
319 Here we calculated the adequacy for each of the published Hg time series in tropical tunas and reveal
320 that only two of the five were statistically powerful (Figure 5). This result highlights the urgent need
321 for long and continuous monitoring programs of Hg concentrations in tunas at these two locations, as

322 well as in other regions of the global ocean to explore the potential time lags between potential
323 changes in Hg emissions to the atmosphere and MeHg levels in marine food webs.

324 Overall, global Hg temporal data in tunas remain too limited in time (i.e., short and/or
325 discontinuous time series) and space (i.e., only two sites) to be able to state whether or not tunas are
326 capable of reflecting the temporal variability of Hg exposure in their ecosystem, at both regional and
327 global scales. Nevertheless, preliminary results, which contrast among ocean regions, and in particular
328 between hemispheres, highlight distinct regional ocean patterns of Hg anthropogenic inputs and
329 deposition, and suggest different responses to changes in emissions given the complex biogeochemical
330 processes governing the speciation, bioavailability, and biomagnification of Hg in the ocean.

331



332

333 **Figure 5. Statistical power of published time series of mercury concentrations in tunas in the global ocean.**
334 Adequacy values of mercury (Hg) time series data in skipjack (diamonds), yellowfin (dots), and bigeye (triangles)
335 in the central north (blue, from Drevnick and Brooks, 2017) and the southwestern (orange, from Médiéu et al.,
336 2021a) Pacific Ocean. Adequacy was calculated following the methods of Bignert et al. (2004), considering a
337 significance level of $p < 0.05$ and 80 % statistical power. Datasets falling within the lower right portion of the
338 graph are more than adequate to detect a 5 % annual change in Hg concentrations, while those in the upper left
339 portion are inadequate.

340

341 **6. Guidelines for collecting and reporting relevant monitoring information on mercury** 342 **in tunas**

343 6.1. Data collection, reporting and organization

344 The use of tuna Hg data to evaluate the effectiveness of the Minamata Convention at reducing
345 Hg emissions requires worldwide collaboration and coordination, framed around a scientifically sound
346 strategy, based on transparent processes, harmonized methodologies, with reliable and comparable
347 datasets. Among all studies documenting Hg concentrations in tunas, less than 13 % (7 over 56) provide
348 all the necessary information for a relevant Hg biomonitoring. Below, we therefore provide
349 recommendations and guidelines for collecting and reporting relevant information on tunas (Figure 6)
350 to monitor tuna MeHg concentrations within an interdisciplinary framework, at both regional and
351 global spatio-temporal patterns, while taking into account possible biological and ecological
352 confounding effects.

353 Precise coordinates and date of capture: To be able to investigate spatial and temporal variability of
354 Hg concentrations in tunas at a high resolution, it is crucial to collect the precise date and location of
355 the tuna fishing operation. Collecting such information is quite easy onboard scientific vessels, as well
356 as on commercial fishing vessels thanks to onboard observers involved in the several sampling
357 programs deployed in the global ocean by regional fishery management organizations. Conversely,
358 fishing information of tuna captured by the artisanal fishery and sampled at the landing can be difficult
359 to obtain. In this case, rather than attributing tuna samples to the port where they were collected, we
360 suggest estimating fishing date and area based on the expertise of the fishermen, or if available, on
361 geo-localised data of the fishing trip (e.g., vessel monitoring system, VMS). Tuna sampling at the
362 market is not adequate for an accurate spatio-temporal Hg biomonitoring as the origin of tuna (i.e.,
363 fishing date and coordinates) is difficult to obtain.

364 Tuna individual straight fork length: Given the natural bioaccumulative property of MeHg in organisms
365 through time, it is necessary to have biological information associated to tuna samples when exploring
366 Hg patterns in tunas. Individual tuna age is the most appropriate biological data to account for
367 bioaccumulation through time; yet it is rarely used because of the inherent uncertainty in tuna ageing
368 methods (e.g., growth models, tagging, interpretation of calcified structures, or analysis of length-
369 frequency data) (Murua et al., 2017). Tuna length and weights therefore represent a good alternative
370 to account for Hg bioaccumulation in individuals. While individual length can be easily measured either
371 onboard or at the lab, precise fish weight cannot be obtained onboard because boats are not stable
372 enough. For a homogeneous and global Hg biomonitoring program with tunas, we therefore
373 recommend measuring individual straight fork length, i.e. from the tip of tuna snout to the fork of the
374 tail (Figure 6), which is the most common and best fitted biometric for fish species like tunas that have
375 forked caudal fins (avoid curved fork length, total length, and standard length).

376 Muscle tissue collection: There are many possible matrices for biomonitoring and tissue choice
377 depends on monitoring objectives, interests, and outcomes. In high trophic level fish species like tunas,
378 it is recommended to monitor MeHg exposure in muscle tissues as i) MeHg is the dominant chemical
379 form (> 90 %, SI Appendix Table S1) in tuna muscle, and ii) muscle is the most edible part of tunas (UN
380 Environment, 2019). Given red muscle exhibits significantly higher total Hg concentrations than white
381 muscle (Bosch et al., 2016), it is important to collect only white muscle tissue during tuna sampling.
382 For homogeneity, we recommend collecting white muscle samples in dorsal position (Figure 6) to
383 account for possible variable lipid contents in different muscle parts among tuna species and ocean
384 regions. If not possible (e.g., no permission to collect samples in dorsal position from fishermen),
385 muscle samples can be alternatively collected in anal position. No difference in total Hg, MeHg and
386 inorganic Hg concentrations were found between dorsal and anal white muscles of yellowfin caught
387 off south Africa (Bosch et al., 2016), yet we suggest first checking for Hg variability between anal and
388 dorsal positions when compiling tuna Hg data obtained in both positions. Tuna muscle samples can be
389 stored in labelled individual cryotubes, plastic zip lock bags, or glass vials. When possible, we advise
390 collecting sufficient amount of muscle tissue without skin (~ 2 g wet weight) in order to anticipate
391 future analyses (e.g., Hg concentrations, stable isotopes, fatty acids, major and trace elements), while
392 taking into account the weight loss after freeze-drying (~ 70 %, SI Appendix Table S1).

393 Other matrices might be interesting to investigate pelagic top predators MeHg exposure, in addition
394 to white muscle tissues. Blood in particular represents a possible non-lethal marker of Hg distribution
395 in tunas, similar to bird and mammal species in other marine ecosystems. While Hg kinetics in tunas

396 remain poorly understood, blood circulation is suspected to play an important role in MeHg
397 distribution across tissues (Leaner and Mason, 2004), and blood is expected to be representative of a
398 short exposure time (~ weeks) compared to muscle tissues (~ months) (Bearhop et al., 2000). In the
399 western central Pacific Ocean, consistency in the spatial distribution patterns of total Hg
400 concentrations in blood and white muscle tissues has been evidenced in yellowfin and bigeye,
401 highlighting the pertinence of these two tissues for large-scale Hg monitoring studies (Barbosa et al.,
402 2022). Such biomonitoring coupling blood and muscle tissues is promising to better understand MeHg
403 accumulation pathway in tunas, and ultimately refine Hg predictions in top predators to address the
404 main challenges of the Minamata Convention.

405 Tissue conservation and preparation prior to analyses: To avoid elements (i.e., Hg, carbon and
406 nitrogen) degradation, white muscle samples must be stored frozen immediately after collection, at
407 minimum -20°C. Also, to avoid concern about variable moisture content, we recommend freeze-drying
408 muscle samples during 48-72h (depending on the amount of tissue collected), instead of drying
409 samples at 60°C, to obtain and compare Hg concentrations on a dry weight basis, as recommended by
410 the Global Mercury Assessment (UN Environment, 2019). At this stage and when possible, we advise
411 estimating gravimetrically the percentage of moisture (i.e., water content), calculating the difference
412 between wet and dry masses of samples after freeze-drying. This allows precise conversion of
413 concentrations from dry weight to wet weight in order to compare tuna Hg concentrations with safety
414 guideline values that are currently expressed on a wet weight basis (FAO Codex Alimentarius
415 Commission, 2021). Otherwise, a mean value of 70 % can be used (SI Appendix Table S1) (Bodin et al.,
416 2017; Houssard et al., 2019; Kojadinovic et al., 2006; Teffer et al., 2014; Vlieg et al., 1993). Finally,
417 muscle samples must be ground into a fine and homogeneous powder to guarantee repeatability and
418 accuracy in lab analyses.

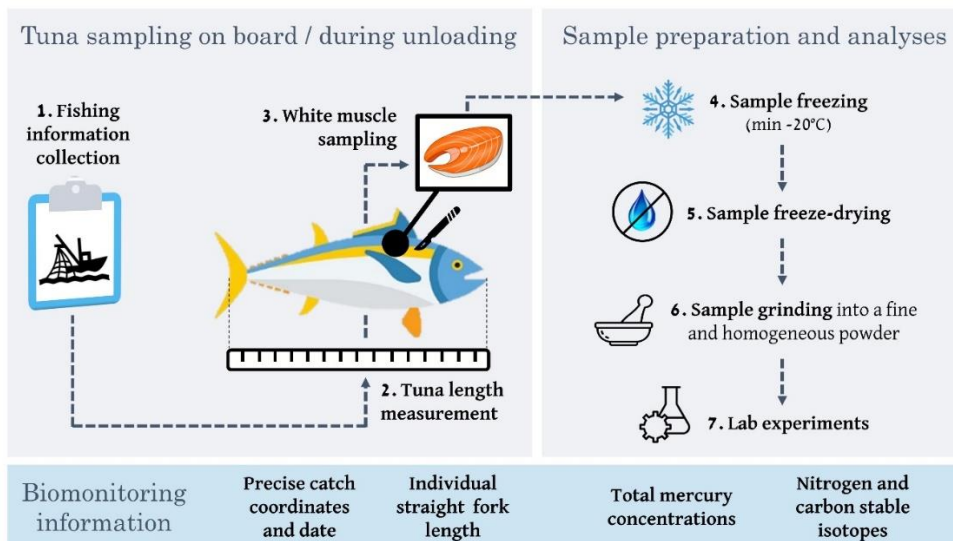
419 Mercury concentrations and ecological tracers: Methylmercury exposure in tuna muscle is
420 recommended to be assessed with total Hg concentrations, as i) MeHg is the dominant chemical form
421 (> 90 %, SI Appendix Table S1) in tuna muscle, and ii) analysis of total Hg concentrations is more cost
422 effective and accessible to those without advanced and costly laboratory facilities (UN Environment,
423 2019). Total Hg concentrations are measured on powdered and homogenized freeze-dried muscle
424 samples by either thermal decomposition, gold amalgamation, and atomic absorption spectrometry,
425 or acid digestion followed by cold vapor atomic fluorescence spectroscopy. Both methods are relevant
426 as long as blanks and biological standard reference materials (e.g., BCR-464, tuna muscle, total Hg =
427 $5240 \pm 100 \text{ ng.g}^{-1}$; TORT-3, lobster hepatopancreas, total Hg = $292 \pm 22 \text{ ng.g}^{-1}$) are routinely used in
428 each analytical batch and reported by authors with the corresponding recoveries to check Hg
429 measurements accuracy and traceability. Total Hg concentrations are expressed on a dry weight basis,
430 and can be converted on a wet weight basis to be compared to safety guidelines values (FAO Codex
431 Alimentarius Commission, 2021).

432 To explore the potential confounding effects of changes in tuna trophic position, habitat, and feeding
433 pathway, we recommend systematically analysing bulk muscle carbon and nitrogen stable isotope
434 values ($\delta^{13}\text{C}$ and $\delta^{15}\text{N}$) in addition to total Hg concentrations. Carbon and nitrogen stable isotopes are
435 measured on powdered and homogenized freeze-dried muscle samples packed in tin cups and
436 analysed with an elemental analyser coupled to an isotope ratio mass spectrometer. Results are
437 reported in the δ unit notation and expressed as part of thousand (‰) relative to international
438 standards. Similar to Hg analyses, a combination of certified and/or in-house reference materials must

439 be used to ensure replication, accuracy, and precision within typical acceptable ranges. Lipid extraction
 440 on a subaliquot of the bulk muscle powder (Hg being measured on the bulk fraction) can be performed
 441 with neutral solvents (e.g., dichloromethane, cyclohexane) prior to $\delta^{13}\text{C}$ analysis to overcome bias
 442 related to lipid content (Bodin et al., 2009; Ménard et al., 2007). On preserved lipid-free samples
 443 initially prepared for tuna foraging ecology (e.g., Bodin et al., 2020) that represent a gold mine of
 444 already collected samples for Hg biomonitoring, it is yet possible to analyse total Hg concentrations as
 445 lipid removal has been shown to have no effect on total Hg concentrations in tropical tunas (Médiéu
 446 et al., 2021b). Another alternative to avoid chemical lipid removal is to measure both total Hg
 447 concentrations and $\delta^{13}\text{C}$ and $\delta^{15}\text{N}$ values on bulk muscle powders, and to correct $\delta^{13}\text{C}$ values in samples
 448 with elevated lipid content ($\text{C:N} > 3.5$), using a mass balance equation mathematical derived from
 449 Atlantic bluefin tuna muscle (Logan et al., 2008).

450 When using tuna $\delta^{15}\text{N}$ ratios to explore possible confounding trophic effects on Hg concentrations, it
 451 is important to keep in mind that tuna $\delta^{15}\text{N}$ values reflect both trophic dynamics along food webs, and
 452 biogeochemical processes at the base of marine food webs (e.g., demand for the nitrogenous nutrients
 453 by primary producers, or variability in the dominant dissolved nitrogen species present; Lorrain et al.,
 454 2015). While this baseline effect may be negligible at a local spatial or temporal scale, it may
 455 significantly bias tuna trophic position estimates when working at larger scales given the large spatial
 456 and temporal variations of $\delta^{15}\text{N}$ baseline signature in the global ocean (McMahon et al., 2013). In
 457 section 8.1, we provide alternatives to better account for baseline variability when exploring the
 458 relative importance of trophic processes on Hg accumulation in tunas.

459



460

461 **Figure 6. Conceptual framework of the standardized guidelines for collecting and reporting relevant**
 462 **monitoring information on tunas.**

463

464 6.2. Data standardization

465 When exploring Hg patterns at both spatial and temporal scales, we recommend standardizing
 466 Hg concentrations to remove the bias associated to fish size differences among individuals, and to
 467 characterize the extent of the natural bioaccumulative processes of Hg in tunas, following the

468 methodology used in three recent studies in the Pacific Ocean (Houssard et al., 2019; Médiéu et al.,
469 2022, 2021a). Briefly, this consists in fitting power-law relationships ($\log(\text{Hg}) = a \times (\text{FL} - b)^c - d$) between
470 log-transformed Hg concentrations and tuna fork length (FL). Residuals from these length-based
471 models (i.e., observed values – predicted values) are extracted and used to calculate length-
472 standardized Hg concentrations at mean species lengths (e.g., 100 cm FL for bigeye, yellowfin and
473 albacore, and 60 cm FL for skipjack), thereafter defined as “standardized Hg concentrations”, in
474 contrast to “observed Hg concentrations”. Such standardization at fish length allows the exploration
475 of spatial and temporal Hg patterns within a same tuna species, as evidenced in sections 4 and 5
476 respectively, but also inter-species differences to explore different Hg accumulation pathways in
477 relation to tuna foraging depths (section 2).

478 For an accurate global comparison of Hg concentrations in tunas, age-standardization, rather
479 that length-standardization, might be more relevant given that tuna growth varies among ocean basins
480 (Murua et al., 2017; Tseng et al., 2021). To do so, power-law relationship can be fit between logHg and
481 tuna age, with tuna age estimated from tuna fork length using species- and ocean- specific growth
482 models, as recommended by fisheries scientists for tuna stock assessments. Nevertheless, given the
483 uncertainties related to tuna growth models and the resulting potential bias on age estimations, we
484 assume that length-standardization of Hg concentrations remains relevant to explore spatio-temporal
485 variability of tuna Hg content when working at small or large regional scales.

486

487 **7. Caveats and limitations**

488 Being highly exploited worldwide and monitored by extensive regional fishery management
489 organizations, tropical tunas and albacore represent a possible gold mine of biological samples to get
490 robust and comparable Hg datasets, as required for an effective Hg biomonitoring in the context of the
491 Minamata Convention. This sampling strategy provides a considerable gain of time, effort, and cost for
492 scientists in charge of sample collection. Yet, this implies that the spatial and temporal coverage, as
493 well as the fishing gear and technique rely solely on the fishermen and fishing companies, leading
494 possibly to poorly documented ocean regions, and/or discontinuous Hg time series. This sampling
495 strategy can also induce variability in tuna length resulting for different fishing gear selecting
496 preferentially certain tuna fish sizes. In the eastern Pacific Ocean for instance, fishing companies
497 principally target surface tunas with purse seine, i.e., mainly skipjack, yellowfin and juvenile bigeye
498 (Inter-American Tropical Tuna Commission, 2021), while in the southwestern Pacific Ocean, fishermen
499 preferentially target adult yellowfin and bigeye in deeper waters with longlines (ISSF, 2021). Although
500 the length- (or age-) standardization approach recommended above allows taking into account this
501 spatial variability of fishing gear and tuna length among samples, it is important to keep in mind the
502 biological and ecological consequences of this sampling bias when exploring Hg accumulation in tunas.

503 In addition, while relatively easy to collect, tuna samples remain available for the last few
504 years/decades only, mostly when regional fishery management organizations started to build
505 specimen tissue banks, and the oldest published Hg data are from the 1970s. Contrary to seabirds, it
506 is not possible to analyse historical samples (e.g., feathers) stored in natural history museum
507 collections to obtain historical Hg data. Such biological archives are yet valuable to discuss Hg temporal
508 trends in marine predators in parallel to Hg emissions and deposition trends over a long period of time,
509 and to better assess the impacts of anthropogenic Hg releases on marine ecosystems on multidecadal

510 timescales (e.g., Bond et al., 2015; Carravieri et al., 2016; Monteiro and Furness, 1997). The combined
511 use of body feathers from museum specimens and free-living birds of sooty tern recently highlighted
512 an increase of 58.9 % of mean Hg concentrations between the 1920s and the 2020s, likely reflecting
513 ecosystem-wide changes in the tropical South Atlantic Ocean and/or anthropogenic Hg emissions to
514 the environment (Cusset et al., 2023). Overall, this highlights the need to combine several
515 biomonitoring species to capture large spatial and temporal scales of Hg exposure in different
516 ecosystems.

517

518 **8. Future directions**

519 8.1. Data integration with oceanic and ecological variables

520 In addition to the provision of information listed above, other metadata are relevant to
521 interpret tuna Hg concentrations regarding possible confounding changes in tuna trophic ecology, and
522 ultimately to predict Hg concentrations in tunas according to changes in anthropogenic releases.

523 The recent development of global physical and biogeochemical models now allow better
524 quantifying the variability of ocean (thermo-)dynamics and baseline processes, and tracking nutrient
525 flow along marine food webs (e.g., NEMO-PISCES, Buchanan et al., 2021; and MOBI, Somes et al.,
526 2017). Such models, providing baseline $\delta^{13}\text{C}$ and in particular $\delta^{15}\text{N}$ estimates in phytoplankton for each
527 tuna Hg data location, offer new perspectives to take into account natural baseline processes while
528 exploring the relative importance of trophic factors on Hg variability in tunas. In the Pacific Ocean for
529 instance, both estimated $\delta^{15}\text{N}$ values in particulate organic matter, and baseline-corrected tuna $\delta^{15}\text{N}$
530 values (i.e., difference of $\delta^{15}\text{N}$ values in tunas and particulate organic matter) helped disentangling the
531 relative importance of baseline and trophic processes, respectively when explaining the large spatial
532 patterns of standardized Hg concentrations in skipjack (Médieu et al., 2022).

533 Moreover, developing simulations of MeHg concentrations in seawater and
534 phyto/zooplankton by global 3-D models (e.g., MITgcm, Zhang et al., 2020) can offer new alternatives
535 to the scarce observations of Hg concentrations and speciation in the ocean to explore global patterns
536 of tuna Hg concentrations alongside regional changes in MeHg production, bioavailability, and
537 biomagnification. Physical and biogeochemical models have been shown to be other relevant tools to
538 investigate the mechanisms governing MeHg bioavailability in seawater. The complementary use of
539 standardized tuna Hg concentrations alongside biogeochemical (e.g., subsurface dissolved O_2
540 concentrations) and physical (e.g., depth of oxycline) model outputs already evidenced the importance
541 of marine biogeochemical processes, in particular variable vertical profiles of dissolved MeHg
542 concentrations among ocean regions, to explain large spatial patterns of tuna Hg concentrations
543 (section 4) (Houssard et al., 2019; Médieu et al., 2022).

544 Finally, atmospheric Hg models represent a good alternative to missing high-resolution and
545 worldwide observed Hg data in the atmosphere to explore tuna Hg concentrations in parallel to
546 changes in anthropogenic Hg emissions and Hg concentrations in the atmosphere. Recently, the
547 complementary use of tuna standardized Hg concentrations alongside atmospheric elemental Hg
548 concentrations predicted by the GEOS-Chem model (Angot et al., 2018; Travnikov et al., 2017) at each
549 tuna location revealed the relationship between actual Asian Hg emissions on elevated skipjack Hg
550 concentrations in the northwestern Pacific Ocean (Médieu et al., 2022).

551 While the use of biological, physical, and anthropogenic model outputs in parallel to
552 standardized Hg concentrations in tunas is promising to improve our understanding of the main
553 processes driving the spatio-temporal variability of Hg content in pelagic top predators, it remains
554 important to keep collecting measurements of Hg concentrations and speciation in the atmosphere
555 and the ocean at large spatial and temporal scales in contrasted tropical regions. The comparison of
556 these observations data with standardized Hg concentrations in tunas, as done in recent studies
557 (Barbosa et al., 2022; Tseng et al., 2021), is indeed crucial to validate the main hypotheses formulated
558 with model outputs, and to refine predictions of Hg responses in pelagic biota to the different
559 emissions and climate change scenarios of the Minamata Convention.

560

561 8.2. Mercury stable isotopes

562 Among the elemental and molecular analytical tools available to explore the Hg cycle, Hg stable
563 isotope signatures measured in biotic tissues has improved significantly our understanding of the
564 biogeochemical, ecological, and metabolic factors driving MeHg exposure. Thanks to the unique
565 photochemical mass-independent fractionation of Hg isotopes (reported as $\Delta^{199}\text{Hg}$), it is now possible
566 to trace trophic resources and the vertical foraging habitat of pelagic species (Le Croizier et al., 2020;
567 Madigan et al., 2018). Following light attenuation with depth, $\Delta^{199}\text{Hg}$ values decrease from the surface
568 to the aphotic waters (Blum et al., 2013), but are conserved during trophic transfer between a prey
569 and its predator (Kwon et al., 2016; Laffont et al., 2011), leading to lower $\Delta^{199}\text{Hg}$ values in deeper
570 marine predators. Mercury stable isotopes also offer new perspectives to investigate how climate
571 change can affect MeHg concentrations in marine food webs. In the Arctic, $\Delta^{199}\text{Hg}$ values in marine
572 biological samples showed the influence of sea ice on Hg photodegradation (Point et al., 2011), and
573 documented the effect of climate change of Hg cycle (Masbou et al., 2015). In tropical ecosystems, the
574 combined use of Hg concentrations, and carbon, nitrogen and Hg stable isotopes, alongside
575 biogeochemical model outputs in seabirds in the northern Humboldt current system off Peru revealed
576 that stable Hg concentrations over time were masking concomitant reduced MeHg formation (due to
577 the deepening of the oxycline) and degradation (due to reduced productivity, carbon export, and
578 remineralization) (Renedo et al., 2021). Similar studies using the global tuna tissue bank are therefore
579 of interest to investigate anthropogenic- and climate-induced changes of MeHg formation,
580 degradation, and accumulation in pelagic marine food webs of tropical ecosystems, at both regional
581 and global scales.

582

583 **Acknowledgements:** We are grateful to research communities working on tuna trophic ecology,
584 mercury cycle and biogeochemical modeling who indirectly contributed to this work. We also thank
585 Anders Bignert from the Swedish Museum of Natural History for the adequacy calculation. This study
586 benefited from thoughtful comments from two anonymous referees.

587 **Funding:** This study was conducted in the framework of ANR-17-CE34-0010 MERTOX (unravelling the
588 origin of methylmercury TOXin in marine ecosystems, 2017 – 2021, PI David Point) from the French
589 Agence Nationale de la Recherche. It also benefited from financial support of the Région Bretagne and
590 Université de Bretagne Occidentale (UBO).

591 **References**

- 592 AMAP, 2021. AMAP Assessment 2021: Mercury in the Arctic. Arctic Monitoring and Assessment
 593 (AMAP). Tromso, Norway.
- 594 Angot, H., Hoffman, N., Giang, A., Thackray, C.P., Hendricks, A.N., Urban, N.R., Selin, N.E., 2018.
 595 Global and Local Impacts of Delayed Mercury Mitigation Efforts. *Environ. Sci. Technol.* 52,
 596 12968–12977. <https://doi.org/10.1021/acs.est.8b04542>
- 597 Axelrad, D.A., Bellinger, D.C., Ryan, L.M., Woodruff, T.J., 2007. Dose–Response Relationship of
 598 Prenatal Mercury Exposure and IQ: An Integrative Analysis of Epidemiologic Data.
 599 *Environmental Health Perspectives* 115, 609–615. <https://doi.org/10.1289/ehp.9303>
- 600 Barbosa, R.V., Point, D., Médiéu, A., Allain, V., Gillikin, D.P., Couturier, L.I.E., Munaron, J.-M.,
 601 Rroupsard, F., Lorrain, A., 2022. Mercury concentrations in tuna blood and muscle mirror
 602 seawater methylmercury in the Western and Central Pacific Ocean. *Marine Pollution Bulletin*
 603 180, 113801. <https://doi.org/10.1016/j.marpolbul.2022.113801>
- 604 Bearhop, S., Ruxton, G.D., Furness, R.W., 2000. Dynamics of mercury in blood and feathers of great
 605 skuas. *Environmental Toxicology and Chemistry* 19, 1638–1643.
 606 <https://doi.org/10.1002/etc.5620190622>
- 607 Bell, J.D., Kronen, M., Vunisea, A., Nash, W.J., Keeble, G., Demmke, A., Pontifex, S., Andréfouët, S.,
 608 2009. Planning the use of fish for food security in the Pacific. *Marine Policy* 33, 64–76.
 609 <https://doi.org/10.1016/j.marpol.2008.04.002>
- 610 Bellanger, M., Pichery, C., Aerts, D., Berglund, M., Castaño, A., Čejchanová, M., Crettaz, P., Davidson,
 611 F., Esteban, M., Fischer, M.E., Gurzau, A.E., Halzlova, K., Katsonouri, A., Knudsen, L.E.,
 612 Kolossa-Gehring, M., Koppen, G., Ligocka, D., Miklavčič, A., Reis, M., ccccFátima, Rudnai, P.,
 613 Tratnik, J.S., Weihe, P., Budtz-Jørgensen, E., Grandjean, P., DEMO/COPHES, 2013. Economic
 614 benefits of methylmercury exposure control in Europe: Monetary value of neurotoxicity
 615 prevention. *Environmental Health* 12, 3. <https://doi.org/10.1186/1476-069X-12-3>
- 616 Béné, C., Barange, M., Subasinghe, R., Pinstrop-Andersen, P., Merino, G., Hemre, G.-I., Williams, M.,
 617 2015. Feeding 9 billion by 2050 – Putting fish back on the menu. *Food Sec.* 7, 261–274.
 618 <https://doi.org/10.1007/s12571-015-0427-z>
- 619 Besada, V., 2006. Mercury, cadmium, lead, arsenic, copper and zinc concentrations in albacore,
 620 yellowfin tuna and bigeye tuna from the Atlantic Ocean. *Ciencias Marinas* 32, 439–445.
 621 <https://doi.org/10.7773/cm.v32i22.1083>
- 622 Bignert, A., Riget, F., Braune, B., Outridge, P., Wilson, S., 2004. Recent temporal trend monitoring of
 623 mercury in Arctic biota – how powerful are the existing data sets? *J. Environ. Monit.* 6, 351–
 624 355. <https://doi.org/10.1039/B312118F>
- 625 Block, B.A., Teo, S.L.H., Walli, A., Boustany, A., Stokesbury, M.J.W., Farwell, C.J., Weng, K.C., Dewar,
 626 H., Williams, T.D., 2005. Electronic tagging and population structure of Atlantic bluefin tuna.
 627 *Nature* 434, 1121–1127. <https://doi.org/10.1038/nature03463>
- 628 Blum, J.D., Popp, B.N., Drazen, J.C., Anela Choy, C., Johnson, M.W., 2013. Methylmercury production
 629 below the mixed layer in the North Pacific Ocean. *Nature Geoscience* 6, 879–884.
 630 <https://doi.org/10.1038/ngeo1918>
- 631 Bodin, N., Budzinski, H., Le Ménach, K., Tapie, N., 2009. ASE extraction method for simultaneous
 632 carbon and nitrogen stable isotope analysis in soft tissues of aquatic organisms. *Analytica*
 633 *Chimica Acta* 643, 54–60. <https://doi.org/10.1016/j.aca.2009.03.048>
- 634 Bodin, N., Lesperance, D., Albert, R., Hollanda, S., Michaud, P., Degroote, M., Churlaud, C.,
 635 Bustamante, P., 2017. Trace elements in oceanic pelagic communities in the western Indian
 636 Ocean. *Chemosphere* 174, 354–362. <https://doi.org/10.1016/j.chemosphere.2017.01.099>
- 637 Bodin, N., Pethybridge, H., Duffy, L.M., Lorrain, A., Allain, V., Logan, J.M., Ménard, F., Graham, B.,
 638 Choy, C.A., Somes, C.J., Olson, R.J., Young, J.W., 2020. Global data set for nitrogen and
 639 carbon stable isotopes of tunas. *Ecology*. <https://doi.org/10.1002/ecy.3265>

640 Bond, A.L., Hobson, K.A., Branfireun, B.A., 2015. Rapidly increasing methyl mercury in endangered
641 ivory gull (*Pagophila eburnea*) feathers over a 130 year record. *Proceedings of the Royal*
642 *Society B: Biological Sciences* 282, 20150032. <https://doi.org/10.1098/rspb.2015.0032>

643 Bosch, A.C., O'Neill, B., Sigge, G.O., Kerwath, S.E., Hoffman, L.C., 2016. Mercury accumulation in
644 Yellowfin tuna (*Thunnus albacares*) with regards to muscle type, muscle position and fish
645 size. *Food Chemistry* 190, 351–356. <https://doi.org/10.1016/j.foodchem.2015.05.109>

646 Boush, G.M., Thieleke, J.R., 1983. Total mercury content in yellowfin and bigeye tuna. *Bull. Environ.*
647 *Contam. Toxicol.* 30, 291–297. <https://doi.org/10.1007/BF01610135>

648 Bowman, K.L., Lamborg, C.H., Agather, A.M., 2020. A global perspective on mercury cycling in the
649 ocean. *Science of The Total Environment* 710, 136166.
650 <https://doi.org/10.1016/j.scitotenv.2019.136166>

651 Buchanan, P.J., Aumont, O., Bopp, L., Mahaffey, C., Tagliabue, A., 2021. Impact of intensifying
652 nitrogen limitation on ocean net primary production is fingerprinted by nitrogen isotopes.
653 *Nat Commun* 12, 6214. <https://doi.org/10.1038/s41467-021-26552-w>

654 Cai, Y., Rooker, J.R., Gill, G.A., Turner, J.P., 2007. Bioaccumulation of mercury in pelagic fishes from
655 the northern Gulf of Mexico. *Canadian Journal of Fisheries and Aquatic Sciences* 64, 458–469.
656 <https://doi.org/10.1139/f07-017>

657 Carravieri, A., Cherel, Y., Jaeger, A., Churlaud, C., Bustamante, P., 2016. Penguins as bioindicators of
658 mercury contamination in the southern Indian Ocean: geographical and temporal trends.
659 *Environmental Pollution* 213, 195–205. <https://doi.org/10.1016/j.envpol.2016.02.010>

660 Chen, C.-Y., Lai, C.-C., Chen, K.-S., Hsu, C.-C., Hung, C.-C., Chen, M.-H., 2014. Total and organic
661 mercury concentrations in the muscles of Pacific albacore (*Thunnus alalunga*) and bigeye
662 tuna (*Thunnus obesus*). *Marine Pollution Bulletin* 85, 606–612.
663 <https://doi.org/10.1016/j.marpolbul.2014.01.039>

664 Chen, M.H., Teng, P.Y., Chen, C.Y., Hsu, C.C., 2011. Organic and total mercury levels in bigeye tuna,
665 *Thunnus obesus*, harvested by Taiwanese fishing vessels in the Atlantic and Indian Oceans.
666 *Food Additives and Contaminants: Part B* 4, 15–21.
667 <https://doi.org/10.1080/19393210.2010.535908>

668 Chouvelon, T., Brach-Papa, C., Auger, D., Bodin, N., Bruzac, S., Crochet, S., Degroote, M., Hollanda,
669 S.J., Hubert, C., Knoery, J., Munschy, C., Puech, A., Rozuel, E., Thomas, B., West, W., Bourjea,
670 J., Nikolic, N., 2017. Chemical contaminants (trace metals, persistent organic pollutants) in
671 albacore tuna from western Indian and south-eastern Atlantic Oceans: Trophic influence and
672 potential as tracers of populations. *Science of The Total Environment* 596–597, 481–495.
673 <https://doi.org/10.1016/j.scitotenv.2017.04.048>

674 Choy, C.A., Popp, B.N., Kaneko, J.J., Drazen, J.C., 2009. The influence of depth on mercury levels in
675 pelagic fishes and their prey. *Proceedings of the National Academy of Sciences* 106, 13865–
676 13869. <https://doi.org/10.1073/pnas.0900711106>

677 Cusset, F., Reynolds, S.J., Carravieri, A., Amouroux, D., Asensio, O., Dickey, R.C., Fort, J., Hughes, B.J.,
678 Paiva, V.H., Ramos, J.A., Shearer, L., Tessier, E., Wearn, C.P., Cherel, Y., Bustamante, P., 2023.
679 A century of mercury: Ecosystem-wide changes drive increasing contamination of a tropical
680 seabird species in the South Atlantic Ocean. *Environmental Pollution* 121187.
681 <https://doi.org/10.1016/j.envpol.2023.121187>

682 Drevnick, P.E., Brooks, B.A., 2017. Mercury in tunas and blue marlin in the North Pacific Ocean.
683 *Environmental Toxicology and Chemistry* 36, 1365–1374. <https://doi.org/10.1002/etc.3757>

684 Drevnick, P.E., Lamborg, C.H., Horgan, M.J., 2015. Increase in mercury in Pacific yellowfin tuna:
685 Mercury in yellowfin tuna. *Environ Toxicol Chem* 34, 931–934.
686 <https://doi.org/10.1002/etc.2883>

687 Endo, T., Kimura, O., Fujii, Y., Haraguchi, K., 2016. Relationship between mercury, organochlorine
688 compounds and stable isotope ratios of carbon and nitrogen in yellowfin tuna (*Thunnus*
689 *albacares*) taken from different regions of the Pacific and Indian Oceans. *Ecological Indicators*
690 69, 340–347. <https://doi.org/10.1016/j.ecolind.2016.04.021>

691 FAO (Ed.), 2018. The state of world fisheries and aquaculture 2018 - Meeting the sustainable
692 development goals. Rome.

693 FAO Codex Alimentarius Commission, 2021. Working document for information and use in
694 discussions related to contaminants and toxins in the GSCTFF [WWW Document]. URL
695 [https://www.fao.org/fao-who-codexalimentarius/sh-](https://www.fao.org/fao-who-codexalimentarius/sh-proxy/en/?lnk=1&url=https%253A%252F%252Fworkspace.fao.org%252Fsites%252Fcodex%252FMeetings%252FCX-735-14%252FINFO-DOC%252FCF14_INF01x.pdf)
696 [proxy/en/?lnk=1&url=https%253A%252F%252Fworkspace.fao.org%252Fsites%252Fcodex%252FMeetings%252FCX-735-14%252FINFO-DOC%252FCF14_INF01x.pdf](https://www.fao.org/fao-who-codexalimentarius/sh-proxy/en/?lnk=1&url=https%253A%252F%252Fworkspace.fao.org%252Fsites%252Fcodex%252FMeetings%252FCX-735-14%252FINFO-DOC%252FCF14_INF01x.pdf) (accessed 12.20.22).
697

698 Ferriss, B.E., Essington, T.E., 2011. Regional patterns in mercury and selenium concentrations of
699 yellowfin tuna (*Thunnus albacares*) and bigeye tuna (*Thunnus obesus*) in the Pacific Ocean.
700 *Can. J. Fish. Aquat. Sci.* 68, 2046–2056. <https://doi.org/10.1139/f2011-120>

701 Fonteneau, A., Hallier, J.-P., 2015. Fifty years of dart tag recoveries for tropical tuna: A global
702 comparison of results for the western Pacific, eastern Pacific, Atlantic, and Indian Oceans.
703 *Fisheries Research* 163, 7–22. <https://doi.org/10.1016/j.fishres.2014.03.022>

704 Garcia, N., Raimbault, P., Sandroni, V., 2007. Seasonal nitrogen fixation and primary production in the
705 Southwest Pacific: nanoplankton diazotrophy and transfer of nitrogen to picoplankton
706 organisms. *Mar. Ecol. Prog. Ser.* 343, 25–33. <https://doi.org/10.3354/meps06882>

707 Garcia-Vazquez, E., Geslin, V., Turrero, P., Rodriguez, N., Machado-Schiaffino, G., Ardura, A., 2021.
708 Oceanic karma? Eco-ethical gaps in African EEE metal cycle may hit back through seafood
709 contamination. *Science of The Total Environment* 762, 143098.
710 <https://doi.org/10.1016/j.scitotenv.2020.143098>

711 Genchi, G., Sinicropi, M., Carocci, A., Lauria, G., Catalano, A., 2017. Mercury Exposure and Heart
712 Diseases. *IJERPH* 14, 74. <https://doi.org/10.3390/ijerph14010074>

713 Hobday, A., Evans, K., Eveson, J.P., Farley, J., Hartog, J., Basson, M., Patterson, T., 2015. Distribution
714 and Migration—Southern Bluefin Tuna (*Thunnus maccoyii*), in: *Biology and Ecology of Bluefin*
715 *Tuna*. pp. 189–210. <https://doi.org/10.1201/b18714-12>

716 Horowitz, H.M., Jacob, D.J., Zhang, Y., Dibble, T.S., Slemr, F., Amos, H.M., Schmidt, J.A., Corbitt, E.S.,
717 Marais, E.A., Sunderland, E.M., 2017. A new mechanism for atmospheric mercury redox
718 chemistry: implications for the global mercury budget. *Atmospheric Chemistry and Physics*
719 17. <https://doi.org/10.5194/acp-17-6353-2017>

720 Houssard, P., Lorrain, A., Tremblay-Boyer, L., Allain, V., Graham, B.S., Menkes, C.E., Pethybridge, H.,
721 Couturier, L.I.E., Point, D., Leroy, B., Receveur, A., Hunt, B.P.V., Vourey, E., Bonnet, S., Rodier,
722 M., Raimbault, P., Feunteun, E., Kuhnert, P.M., Munaron, J.-M., Lebreton, B., Otake, T.,
723 Letourneur, Y., 2017. Trophic position increases with thermocline depth in yellowfin and
724 bigeye tuna across the Western and Central Pacific Ocean. *Progress in Oceanography* 154,
725 49–63. <https://doi.org/10.1016/j.pocean.2017.04.008>

726 Houssard, P., Point, D., Tremblay-Boyer, L., Allain, V., Pethybridge, H., Masbou, J., Ferriss, B.E., Baya,
727 P.A., Lagane, C., Menkes, C.E., Letourneur, Y., Lorrain, A., 2019. A Model of Mercury
728 Distribution in Tuna from the Western and Central Pacific Ocean: Influence of Physiology,
729 Ecology and Environmental Factors. *Environmental Science & Technology* 53, 1422–1431.
730 <https://doi.org/10.1021/acs.est.8b06058>

731 Inter-American Tropical Tuna Commission, 2021. Report on the tuna fishery, stocks, and ecosystem
732 in the eastern Pacific Ocean in 2020 (No. IATTC-98-01).

733 ISSF, 2021. Status of the World Fisheries for Tuna: March 2021 (ISSF Technical Report 2021-10).
734 International Seafood Sustainability Foundation, Washington, D.C., USA.

735 IUCN, 2017. The IUCN Red List of Threatened Species [WWW Document]. IUCN Red List of
736 Threatened Species. URL <https://www.iucnredlist.org/en> (accessed 10.25.21).

737 Jiskra, M., Sonke, J.E., Lim, A.G., Loiko, S.V., Kosykh, N., Pokrovsky, O., Agnan, Y., Helmig, D., Obrist,
738 D., 2020. The role of permafrost soils in Arctic mercury cycling: source tracing with Hg stable
739 isotopes and revised soil pool estimate 5734. [https://doi.org/10.5194/egusphere-egu2020-](https://doi.org/10.5194/egusphere-egu2020-5734)
740 5734

741 Kojadinovic, J., Potier, M., Le Corre, M., Cosson, R.P., Bustamante, P., 2007. Bioaccumulation of trace
742 elements in pelagic fish from the Western Indian Ocean. *Environmental Pollution, Lichens in*

743 a Changing Pollution Environment 146, 548–566.
744 <https://doi.org/10.1016/j.envpol.2006.07.015>

745 Kojadinovic, J., Potier, M., Le Corre, M., Cosson, R.P., Bustamante, P., 2006. Mercury content in
746 commercial pelagic fish and its risk assessment in the Western Indian Ocean. *Science of The*
747 *Total Environment* 366, 688–700. <https://doi.org/10.1016/j.scitotenv.2006.02.006>

748 Kraepiel, A.M.L., Keller, K., Chin, H.B., Malcolm, E.G., Morel, F.M.M., 2003. Sources and Variations of
749 Mercury in Tuna. *Environmental Science & Technology* 37, 5551–5558.
750 <https://doi.org/10.1021/es0340679>

751 Kwon, S.Y., Blum, J.D., Madigan, D.J., Block, B.A., Popp, B.N., 2016. Quantifying mercury isotope
752 dynamics in captive Pacific bluefin tuna (*Thunnus orientalis*). *Elem Sci Anth* 4, 000088.
753 <https://doi.org/10.12952/journal.elementa.000088>

754 Laffont, L., Sonke, J.E., Maurice, L., Monrroy, S.L., Chincheros, J., Amouroux, D., Behra, P., 2011. Hg
755 Speciation and Stable Isotope Signatures in Human Hair As a Tracer for Dietary and
756 Occupational Exposure to Mercury. *Environ. Sci. Technol.* 45, 9910–9916.
757 <https://doi.org/10.1021/es202353m>

758 Lamborg, C.H., Hammerschmidt, C.R., Bowman, K.L., Swarr, G.J., Munson, K.M., Ohnemus, D.C., Lam,
759 P.J., Heimbürger, L.-E., Rijkenberg, M.J.A., Saito, M.A., 2014. A global ocean inventory of
760 anthropogenic mercury based on water column measurements. *Nature* 512, 65–68.
761 <https://doi.org/10.1038/nature13563>

762 Le Croizier, G., Lorrain, A., Sonke, J.E., Jaquemet, S., Schaal, G., Renedo, M., Besnard, L., Cherel, Y.,
763 Point, D., 2020. Mercury isotopes as tracers of ecology and metabolism in two sympatric
764 shark species. *Environmental Pollution* 265, 114931.
765 <https://doi.org/10.1016/j.envpol.2020.114931>

766 Leaner, J.J., Mason, R.P., 2004. Methylmercury uptake and distribution kinetics in Sheepshead
767 Minnows, *Cyprinodon Variegatus*, after exposure to CH_3Hg -spiked food. *Environ Toxicol*
768 *Chem* 23, 2138. <https://doi.org/10.1897/03-258>

769 Lee, C.-S., Lutcavage, M.E., Chandler, E., Madigan, D.J., Cerrato, R.M., Fisher, N.S., 2016. Declining
770 Mercury Concentrations in Bluefin Tuna Reflect Reduced Emissions to the North Atlantic
771 Ocean. *Environmental Science & Technology* 50, 12825–12830.
772 <https://doi.org/10.1021/acs.est.6b04328>

773 Logan, J.M., Jardine, T.D., Miller, T.J., Bunn, S.E., Cunjak, R.A., Lutcavage, M.E., 2008. Lipid corrections
774 in carbon and nitrogen stable isotope analyses: comparison of chemical extraction and
775 modelling methods. *Journal of Animal Ecology* 77, 838–846. <https://doi.org/10.1111/j.1365-2656.2008.01394.x>

776 Lorrain, A., Graham, B.S., Popp, B.N., Allain, V., Olson, R.J., Hunt, B.P.V., Potier, M., Fry, B., Galván-
777 Magaña, F., Menkes, C.E.R., Kaehler, S., Ménard, F., 2015. Nitrogen isotopic baselines and
778 implications for estimating foraging habitat and trophic position of yellowfin tuna in the
779 Indian and Pacific Oceans. *Deep Sea Research Part II: Topical Studies in Oceanography* 113,
780 188–198. <https://doi.org/10.1016/j.dsr2.2014.02.003>

781 Madigan, D.J., Baumann, Z., Carlisle, A.B., Hoen, D.K., Popp, B.N., Dewar, H., Snodgrass, O.E., Block,
782 B.A., Fisher, N.S., 2014. Reconstructing transoceanic migration patterns of Pacific bluefin
783 tuna using a chemical tracer toolbox. *Ecology* 95, 1674–1683. <https://doi.org/10.1890/13-1467.1>

784 Madigan, D.J., Li, M., Yin, R., Baumann, H., Snodgrass, O.E., Dewar, H., Krabbenhoft, D.P., Baumann,
785 Z., Fisher, N.S., Balcom, P., Sunderland, E.M., 2018. Mercury Stable Isotopes Reveal Influence
786 of Foraging Depth on Mercury Concentrations and Growth in Pacific Bluefin Tuna. *Environ.*
787 *Sci. Technol.* 52, 6256–6264. <https://doi.org/10.1021/acs.est.7b06429>

788 Masbou, J., Point, D., Sonke, J.E., Frappart, F., Perrot, V., Amouroux, D., Richard, P., Becker, P.R.,
789 2015. Hg Stable Isotope Time Trend in Ringed Seals Registers Decreasing Sea Ice Cover in the
790 Alaskan Arctic. *Environ. Sci. Technol.* 49, 8977–8985. <https://doi.org/10.1021/es5048446>

791 Mason, R.P., Fitzgerald, W.F., 1990. Alkylmercury species in the equatorial Pacific. *Nature* 347, 457–
792 459. <https://doi.org/10.1038/347457a0>

795 McMahon, K.W., Hamady, L.L., Thorrold, S.R., 2013. Ocean ecogeochemistry: a review.
796 Oceanography and Marine Biology: An Annual Review 327–374.

797 Médieu, A., Point, D., Itai, T., Angot, H., Buchanan, P.J., Allain, V., Fuller, L., Griffiths, S., Gillikin, D.P.,
798 Sonke, J.E., Heimbürger-Boavida, L.-E., Desgranges, M.-M., Menkes, C.E., Madigan, D.J.,
799 Brosset, P., Gauthier, O., Tagliabue, A., Bopp, L., Verheyden, A., Lorrain, A., 2022. Evidence
800 that Pacific tuna mercury levels are driven by marine methylmercury production and
801 anthropogenic inputs. PNAS 119, 8. <https://doi.org/10.1073/pnas.2113032119>

802 Médieu, A., Point, D., Receveur, A., Gauthier, O., Allain, V., Pethybridge, H., Menkes, C.E., Gillikin,
803 D.P., Revill, A.T., Somes, C.J., Collin, J., Lorrain, A., 2021a. Stable mercury concentrations of
804 tropical tuna in the south western Pacific ocean: An 18-year monitoring study. Chemosphere
805 263, 128024. <https://doi.org/10.1016/j.chemosphere.2020.128024>

806 Médieu, A., Sardenne, F., Lorrain, A., Bodin, N., Pazart, C., Le Delliou, H., Point, D., 2021b. Lipid-free
807 tuna muscle samples are suitable for total mercury analysis. Marine Environmental Research
808 169, 105385. <https://doi.org/10.1016/j.marenvres.2021.105385>

809 Ménard, F., Lorrain, A., Potier, M., Marsac, F., 2007. Isotopic evidence of distinct feeding ecologies
810 and movement patterns in two migratory predators (yellowfin tuna and swordfish) of the
811 western Indian Ocean. Marine Biology 153, 141–152. <https://doi.org/10.1007/s00227-007-0789-7>

812

813 Mergler, D., Anderson, H.A., Chan, L.H.M., Mahaffey, K.R., Murray, M., Sakamoto, M., Stern, A.H.,
814 2007. Methylmercury Exposure and Health Effects in Humans: A Worldwide Concern.
815 AMBIO: A Journal of the Human Environment 36, 3–11. [https://doi.org/10.1579/0044-7447\(2007\)36\[3:MEAHEI\]2.0.CO;2](https://doi.org/10.1579/0044-7447(2007)36[3:MEAHEI]2.0.CO;2)

816

817 Monteiro, L.R., Furness, R.W., 1997. Accelerated increase in mercury contamination in north Atlantic
818 mesopelagic food chains as indicated by time series of seabird feathers. Environmental
819 Toxicology and Chemistry 16, 2489–2493. <https://doi.org/10.1002/etc.5620161208>

820 Murua, H., Rodriguez-Marin, E., Neilson, J.D., Farley, J.H., Juan-Jordá, M.J., 2017. Fast versus slow
821 growing tuna species: age, growth, and implications for population dynamics and fisheries
822 management. Rev Fish Biol Fisheries 27, 733–773. <https://doi.org/10.1007/s11160-017-9474-1>

823

824 Nicklisch, S.C.T., Bonito, L.T., Sandin, S., Hamdoun, A., 2017. Mercury levels of yellowfin tuna
825 (*Thunnus albacares*) are associated with capture location. Environmental Pollution 229, 87–
826 93. <https://doi.org/10.1016/j.envpol.2017.05.070>

827 Olson, R.J., Young, J.W., Ménard, F., Potier, M., Allain, V., Goñi, N., Logan, J.M., Galván-Magaña, F.,
828 2016. Chapter Four: Bioenergetics, Trophic Ecology, and Niche Separation of Tunas, in:
829 Advances in Marine Biology. Elsevier, pp. 199–344.
830 <https://doi.org/10.1016/bs.amb.2016.06.002>

831 Ordiano-Flores, A., Galván-Magaña, F., Rosiles-Martínez, R., 2011. Bioaccumulation of Mercury in
832 Muscle Tissue of Yellowfin Tuna, *Thunnus albacares*, of the Eastern Pacific Ocean. Biological
833 Trace Element Research 144, 606–620. <https://doi.org/10.1007/s12011-011-9136-4>

834 Outridge, P.M., Mason, R.P., Wang, F., Guerrero, S., Heimbürger-Boavida, L.E., 2018. Updated Global
835 and Oceanic Mercury Budgets for the United Nations Global Mercury Assessment 2018.
836 Environ. Sci. Technol. 52, 11466–11477. <https://doi.org/10.1021/acs.est.8b01246>

837 Peterson, C.L., Klawe, W.L., Sharp, G.D., 1973. Mercury in tunas: a review. Fishery Bulletin 71, 11.

838 Pethybridge, H., Choy, C.A., Logan, J.M., Allain, V., Lorrain, A., Bodin, N., Somes, C.J., Young, J.,
839 Ménard, F., Langlais, C., Duffy, L., Hobday, A.J., Kuhnert, P., Fry, B., Menkes, C., Olson, R.J.,
840 2018. A global meta-analysis of marine predator nitrogen stable isotopes: Relationships
841 between trophic structure and environmental conditions. Global Ecology and Biogeography
842 27, 1043–1055. <https://doi.org/10.1111/geb.12763>

843 Point, D., Sonke, J.E., Day, R.D., Roseneau, D.G., Hobson, K.A., Vander Pol, S.S., Moors, A.J., Pugh,
844 R.S., Donard, O.F.X., Becker, P.R., 2011. Methylmercury photodegradation influenced by sea-
845 ice cover in Arctic marine ecosystems. Nature Geosci 4, 188–194.
846 <https://doi.org/10.1038/ngeo1049>

847 Renedo, M., Point, D., Sonke, J.E., Lorrain, A., Demarcq, H., Graco, M., Grados, D., Gutiérrez, D.,
848 Médieu, A., Munaron, J.M., Pietri, A., Colas, F., Tremblay, Y., Roy, A., Bertrand, A., Bertrand,
849 S.L., 2021. ENSO Climate Forcing of the Marine Mercury Cycle in the Peruvian Upwelling Zone
850 Does Not Affect Methylmercury Levels of Marine Avian Top Predators. *Environ. Sci. Technol.*
851 55, 15754–15765. <https://doi.org/10.1021/acs.est.1c03861>

852 Rivers, J.B., Pearson, J.E., Shultz, C.D., 1972. Total and organic mercury in marine fish. *Bull. Environ.*
853 *Contam. Toxicol.* 8, 257–266. <https://doi.org/10.1007/BF01684554>

854 Slemr, F., Angot, H., Dommergue, A., Magand, O., Barret, M., Weigelt, A., Ebinghaus, R., Brunke, E.-
855 G., Pfaffhuber, K.A., Edwards, G., Howard, D., Powell, J., Keywood, M., Wang, F., 2015.
856 Comparison of mercury concentrations measured at several sites in the Southern
857 Hemisphere. *Atmospheric Chemistry and Physics* 15, 3125–3133.
858 <https://doi.org/10.5194/acp-15-3125-2015>

859 Slemr, F., Martin, L., Labuschagne, C., Mkololo, T., Angot, H., Magand, O., Dommergue, A., Garat, P.,
860 Ramonet, M., Bieser, J., 2020. Atmospheric mercury in the Southern Hemisphere – Part 1:
861 Trend and inter-annual variations in atmospheric mercury at Cape Point, South Africa, in
862 2007–2017, and on Amsterdam Island in 2012–2017. *Atmos. Chem. Phys.* 20, 7683–7692.
863 <https://doi.org/10.5194/acp-20-7683-2020>

864 Somes, C.J., Schmittner, A., Muglia, J., Oschlies, A., 2017. A Three-Dimensional Model of the Marine
865 Nitrogen Cycle during the Last Glacial Maximum Constrained by Sedimentary Isotopes.
866 *Frontiers in Marine Science* 4. <https://doi.org/10.3389/fmars.2017.00108>

867 Sompongchaiyakul, P., Hantow, J., Sornkrut, S., Sumontha, M., 2008. An Assessment of Mercury
868 Concentration in Fish Tissues Caught from Three Compartments of the Bay of Bengal, The
869 Ecosystem-Based Fishery Management in the Bay of Bengal. Thailand.

870 Streets, D.G., Horowitz, H.M., Jacob, D.J., Lu, Z., Levin, L., ter Schure, A.F.H., Sunderland, E.M., 2017.
871 Total Mercury Released to the Environment by Human Activities. *Environ. Sci. Technol.* 51,
872 5969–5977. <https://doi.org/10.1021/acs.est.7b00451>

873 Streets, D.G., Horowitz, H.M., Lu, Z., Levin, L., Thackray, C.P., Sunderland, E.M., 2019. Five hundred
874 years of anthropogenic mercury: spatial and temporal release profiles. *Environ. Res. Lett.* 14,
875 084004. <https://doi.org/10.1088/1748-9326/ab281f>

876 Sunderland, E.M., Li, M., Bullard, K., 2018. Decadal Changes in the Edible Supply of Seafood and
877 Methylmercury Exposure in the United States. *Environmental Health Perspectives* 126,
878 017006. <https://doi.org/10.1289/EHP2644>

879 Teffer, A.K., Staudinger, M.D., Taylor, D.L., Juanes, F., 2014. Trophic influences on mercury
880 accumulation in top pelagic predators from offshore New England waters of the northwest
881 Atlantic Ocean. *Marine Environmental Research* 101, 124–134.
882 <https://doi.org/10.1016/j.marenvres.2014.09.008>

883 Travnikov, O., Angot, H., Artaxo, P., Bencardino, M., Bieser, J., D’Amore, F., Dastoor, A., De Simone,
884 F., Diéguez, M. del C., Dommergue, A., Ebinghaus, R., Feng, X.B., Gencarelli, C.N., Hedgecock,
885 I.M., Magand, O., Martin, L., Matthias, V., Mashyanov, N., Pirrone, N., Ramachandran, R.,
886 Read, K.A., Ryjkov, A., Selin, N.E., Sena, F., Song, S., Sprovieri, F., Wip, D., Wängberg, I., Yang,
887 X., 2017. Multi-model study of mercury dispersion in the atmosphere: atmospheric processes
888 and model evaluation. *Atmospheric Chemistry and Physics* 17, 5271–5295.
889 <https://doi.org/10.5194/acp-17-5271-2017>

890 Tseng, C.-M., Ang, S.-J., Chen, Y.-S., Shiao, J.-C., Lamborg, C.H., He, X., Reinfelder, J.R., 2021. Bluefin
891 tuna reveal global patterns of mercury pollution and bioavailability in the world’s oceans.
892 *Proceedings of the National Academy of Sciences* 6.

893 UN Environment, 2019. Global mercury assessment 2018.

894 Vlieg, P., Murray, T., Body, D.R., 1993. Nutritional data on six oceanic pelagic fish species from New
895 Zealand waters. *Journal of Food Composition and Analysis* 6, 45–54.
896 <https://doi.org/10.1006/jfca.1993.1006>

897 Wang, F., Outridge, P.M., Feng, X., Meng, B., Heimbürger-Boavida, L.-E., Mason, R.P., 2019. How
898 closely do mercury trends in fish and other aquatic wildlife track those in the atmosphere? -

899 Implications for evaluating the effectiveness of the Minamata Convention. *Science of the*
900 *Total Environment* 674, 58–70. <https://doi.org/10.1016/j.scitotenv.2019.04.101>
901 Yamashita, Y., Omura, Y., Okazaki, E., 2005. Total mercury and methylmercury levels in commercially
902 important fishes in Japan. *Fisheries Sci* 71, 1029–1035. <https://doi.org/10.1111/j.1444->
903 2906.2005.01060.x
904 Zhang, Y., Jacob, D.J., Horowitz, H.M., Chen, L., Amos, H.M., Krabbenhoft, D.P., Slemr, F., St. Louis,
905 V.L., Sunderland, E.M., 2016. Observed decrease in atmospheric mercury explained by global
906 decline in anthropogenic emissions. *Proc Natl Acad Sci USA* 113, 526–531.
907 <https://doi.org/10.1073/pnas.1516312113>
908 Zhang, Y., Soerensen, A.L., Schartup, A.T., Sunderland, E.M., 2020. A Global Model for Methylmercury
909 Formation and Uptake at the Base of Marine Food Webs. *Global Biogeochem. Cycles* 34.
910 <https://doi.org/10.1029/2019GB006348>
911 Zhang, Y., Song, Z., Huang, S., Zhang, P., Peng, Y., Wu, P., Gu, J., Dutkiewicz, S., Zhang, H., Wu, S.,
912 Wang, F., Chen, L., Wang, S., Li, P., 2021. Global health effects of future atmospheric mercury
913 emissions. *Nat Commun* 12, 3035. <https://doi.org/10.1038/s41467-021-23391-7>
914
915